Correlation between observed α decays and changes in neutron or proton skins from parent to daughter nuclei

W. M. Seif,[1,*] N. V. Antonenko,[2,3] G. G. Adamian,[2] and Hisham Anwer[1,4]
[1]*Cairo University, Faculty of Science, Department of Physics, 12613 Giza, Egypt*
[2]*Joint Institute for Nuclear Research, 141980 Dubna, Russia*
[3]*Mathematical Physics Department, Tomsk Polytechnic University, 634050 Tomsk, Russia*
[4]*Physics Department, Zewail City of Science and Technology, Egypt*
(Received 21 August 2017; published 29 November 2017)

The change of proton and neutron skin thicknesses is investigated in nuclei after α decay. The skin thicknesses are self-consistently calculated. The observed α decays lead to relatively large decrease of the proton skin in the daughter nuclei. A large increase of the neutron skin in the daughter nucleus reflects the hindered α decay. This hindrance is related to the decrease of both the Q_α value and the preformation probability in the parent nucleus. For each isotopic chain, the observed half-lives consistently correlate with the change of the proton (neutron) skin thickness, from parent to daughter nuclei.

DOI: 10.1103/PhysRevC.96.054328

I. INTRODUCTION

The experimental work on the proton and neutron density distributions of stable and exotic nuclei is mainly focusing on the measurement of their root-mean-square (rms) radii and neutron skin thicknesses [1]. The thickness of the neutron skin is simply defined by the difference between the neutron and proton rms radii of a nucleus. The neutron skin could be assigned to the difference of the equations of state of the asymmetric nuclear matter [2] inside the nucleus and on its surface. The neutrons-to-protons ratio increases in the surface region of a neutron-rich nucleus. There is a correlation between the neutron skin and the slope of the symmetry energy [3–5], and consequently with the pressure of neutron matter at saturation density. The correlation between the neutron skin thickness in finite nuclei and the reaction mechanism has been extensively studied. For instance, a correlation was reported between the neutron skin thickness and the electric dipole polarizability [6], the isoscalar giant quadrupole [7] and pygmy [8] resonances, the neutron removal cross section [9], the nuclear surface polarization [10,11], and the "scissors" vibrational modes [12] of neutron-rich nuclei. As pointed out, the barrier and subbarrier fusion cross section can be used to probe the neutron skin of the interacting nuclei [13,14].

The stability of neutron-rich nuclei is mainly determined by their ground state properties, like the deformation [15,16], isospin asymmetry [17,18], and shell effects [19,20]. Other factors are the spin and parity assignments to the unpaired nucleon in open shell, as well as the collective vibrational excitations [21–23]. The differences in these properties from parent to daughter nuclei in addition to the released energy define the decay mode. For α decay, the preformation probability of α cluster, its assaulting frequency, and penetration probability are also important to define the half-life time T_α [24–27].

The influences of the neutron skin thickness on the α and cluster decay processes have been addressed in recent studies [28–30]. A common conclusion drawn is that it is important to include the neutron skin thickness in the half-life calculations of α decays. Its effect comes mainly from the differences between the proton and neutron density distributions and its impact on the α-core interaction potential. Although the neutron skin thickness decreases the barrier for α decay, it generally reduces the calculated T_α, indicating a smaller preformation probability [29]. It has been also related to the slope of symmetry energy through cluster radioactivity [28] and the direct proportionality of the slope of symmetry energy to the neutron skin thickness has been confirmed. The influence of the proton skin thickness on the decay process of proton-skinned nuclei has not explicitly investigated yet. This paper aims to find useful pattern in existing data about correlations among proton or neutron skin thickness and α-decay properties. These correlations are primary expected in the isotopic chains. Toward this goal, we investigated the change of the neutron (proton) skin thickness from parent to daughter nuclei and the correlation of this change with the probability of α decay and T_α. The studied isotopic chains cover a wide region of the nuclear chart at which the α decays copiously appear, starting from the trans-tin region and up to the area of heaviest nuclei. Such a study gives us a confidence in the generality of the phenomena revealed. The results obtained are apparently useful for clarifying the stability of yet unknown exotic nuclei against α decay.

The paper is organized as follows. The theoretical framework of calculating proton- and neutron-skin thickness in the frame work of the Hartree-Fock-Bogoliubov (HFB) method is outlined in Sec. II. In Sec. III, the numerical results are presented and discussed. Finally, a brief summary and conclusions are given in Sec. IV.

II. THEORETICAL FRAMEWORK

The HFB approach, based on the Skyrme-like effective interactions, is widely used for describing the ground-state

*wseif@sci.cu.edu.eg

properties of finite nuclei [31]. For instance, the binding energies, nuclear masses, rms charge and matter radii, single-particle energies, and surface thicknesses are extensively studied using Skyrme-HFB calculations. In this approach, the total energy E of a nucleus is obtained by summing the kinetic, Skyrme, and Coulomb contributions,

$$E = \int d\vec{r}[\mathcal{H}_{\text{kin}}(\rho_{p,n},\tau_{p,n};\vec{r}) + \mathcal{H}_{\text{Skyrme}}(\rho_{p,n},\tau_{p,n},J_{p,n};\vec{r}) + \mathcal{H}_{\text{Coul}}(\rho_p;\vec{r})]. \quad (1)$$

Here, $\mathcal{H}_i$ (i = kin, Skyrme, Coul) represent the energy density functionals for the mentioned contributions. These density functionals are defined in terms of the proton (ρ_p) and neutron (ρ_n) local density distributions, and the corresponding kinetic and spin-orbit densities [32]. The proton (neutron) density is given in terms of the single-particle wave functions $\varphi^i_{p(n)}(\sigma)$ and the corresponding occupation numbers $n^i_{p(n)}$ [32,33],

$$\rho_{p(n)}(\vec{r}) = \sum_{i,\sigma} \left|\varphi^i_{p(n)}(\vec{r},\sigma)\right|^2 n^i_{p(n)}. \quad (2)$$

Here, i and σ define the orbital and spin quantum numbers, respectively. The proton (neutron) root-mean-square radius $R^{\text{rms}}_{p(n)}$ is given as

$$R^{\text{rms}}_{p(n)} = \left\langle R^2_{p(n)}\right\rangle^{1/2} = \left(\frac{\int r^2_{p(n)}\rho_{p(n)}(\vec{r})d\vec{r}}{\int \rho_{p(n)}(\vec{r})d\vec{r}}\right)^{1/2}. \quad (3)$$

In momentum ($\hbar k$) space, the nucleon densities are transformed to the form factors

$$F_{p(n)}(k) = 4\pi \int_0^\infty dr\, r^2\, j_0(kr)\, \rho_{p(n)}(r), \quad (4)$$

where j_0 represents the spherical Bessel function of order zero. The proton (neutron) rms radius can be then obtained from the curvature of the form factor in the limit of $k \to 0$ [31],

$$R^{\text{rms}}_{p(n)} = \frac{3}{F_{n(p)}(0)} \left.\frac{d^2F_{p(n)}(k)}{dk^2}\right|_{k=0}. \quad (5)$$

The neutron skin thickness Δ_n can be determined as the difference between the neutron and proton rms radii,

$$\Delta_n(A,Z) = R^{\text{rms}}_n(A,Z) - R^{\text{rms}}_p(A,Z). \quad (6)$$

In the framework of the preformed cluster model, the α-decay half-life can be obtained in terms of the preformation probability (S_α), the assault frequency (ν), and the penetration probability (P) of the emitted α particle as [24,25]

$$T_\alpha = \frac{\hbar \ln 2}{S_\alpha \nu P}. \quad (7)$$

Based on the Wentzel-Kramers-Brillouin (WKB) approximation, the tunneling assault frequency and the penetration probability are given, respectively, by

$$\nu = \left[\int_{R_1}^{R_2} \frac{2\mu}{\hbar k(r)} dr\right]^{-1}, \quad (8)$$

and

$$P = e^{-2\int_{R_2}^{R_3} k(r)dr}, \quad (9)$$

where $k(r) = \sqrt{2\mu|V_T(r) - Q_\alpha|/\hbar^2}$. Q_α and μ and define the energy released in the decay process and the reduced mass of the α-daughter nucleus system, respectively. The classical turning points $R_{i=1,2,3}$(fm) are defined along the tunneling path of the α particle by the condition $V_T(r)|_{r=R_i} = Q_\alpha$. $V_T(r) = V_N + V_C + V_\ell$ represents the total interaction potential between the α particle and the daughter nucleus. In the present work, the nuclear (V_N) and Coulomb (V_C) parts of the interaction potential are calculated using the energy density formalism based on the Skyrme-SLy4 nucleon-nucleon interaction, and the direct and exchange Coulomb functionals [32]. The centrifugal potential (V_ℓ) is calculated in terms of the angular momentum carried by the α particle, in the unfavored decays. The details of the method of calculation are given in Refs. [23,24].

III. RESULTS AND DISCUSSION

Alpha decays are rarely observed in light nuclei. The alpha radioactivity of heavy nuclei starts at $Z = 52$ (^{105}Te). Six tellurium ($^{105-110}$Te), seven iodine ($^{107-113}$I), and six xenon ($^{109-113,115}$Xe) isotopes are known to be α emitters [34,35]. A common feature of these α-emitters and their daughters is that they have proton skins, $\Delta_p = R^{\text{rms}}_p - R^{\text{rms}}_n = -\Delta_n > 0$. Figure 1(a) shows the difference between the proton skin thicknesses of the produced $^{101-106}$Sn, $^{103-109}$Sb, and $^{105-109,111}$Te daughter nuclei and the corresponding skin thicknesses of the $^{105-110}$Te, $^{107-113}$I, and $^{109-113,115}$Xe parent nuclei, respectively, $\delta_{p\alpha} = \Delta_p(A-4,Z-2) - \Delta_p(A,Z)$. In the same figure we also show $\delta_{p\alpha}$ for $^{124-129}$Nd, $^{133-139}$Gd, and $^{148-152}$Yb isotopes, in which no α emissions were observed. The performed calculations rely on the HFB approximation and the energy density functionals Eq. (1) based on the Skyrme-SLy4 interaction [33], using the computer code in Ref. [31]. Both the pairing and shell effects are included in the calculations [33,36]. Figure 1(b) shows the Q_α values [37] for the isotopes presented in Fig. 1(a). The observed partial half-lives (T_α) of the α emitters in Fig. 1(a) are displayed in Fig. 1(c).

The calculated proton skin thickness of the $^{105-110}$Te isotopes steadily decreases from Δ_p (^{105}Te) = 0.075 fm to Δ_p (^{110}Te) = 0.013 fm. The daughter nuclei ($^{101-106}$Sn) produced in the α decays of these isotopes have smaller proton skin thicknesses, the values of $\delta_{p\alpha}$ are relatively large. The relatively large reduction of the proton skin sickness due to the α-emission indicates more stable daughter nucleus. As seen in Figs. 1(a) and 1(c), both the reduction in the proton skin thicknesses after the α emission and the observed partial half-lives $^{105-110}$Te increase with decreasing their proton skins (increasing N). The nucleus ^{111}Te has a very thin proton skin of $\Delta_p = 0.002$ fm and its daughter ^{107}Sn has instead a neutron skin of $\Delta_n = 0.012$ fm. The next $^{112-119}$Te isotopes have neutron skins which systematically increase up to Δ_n (^{119}Te) = 0.078 fm. The daughter (A-4, Z-2) nuclei $^{108-115}$Sn of these isotopes exhibit relatively thicker neutron skins ranging

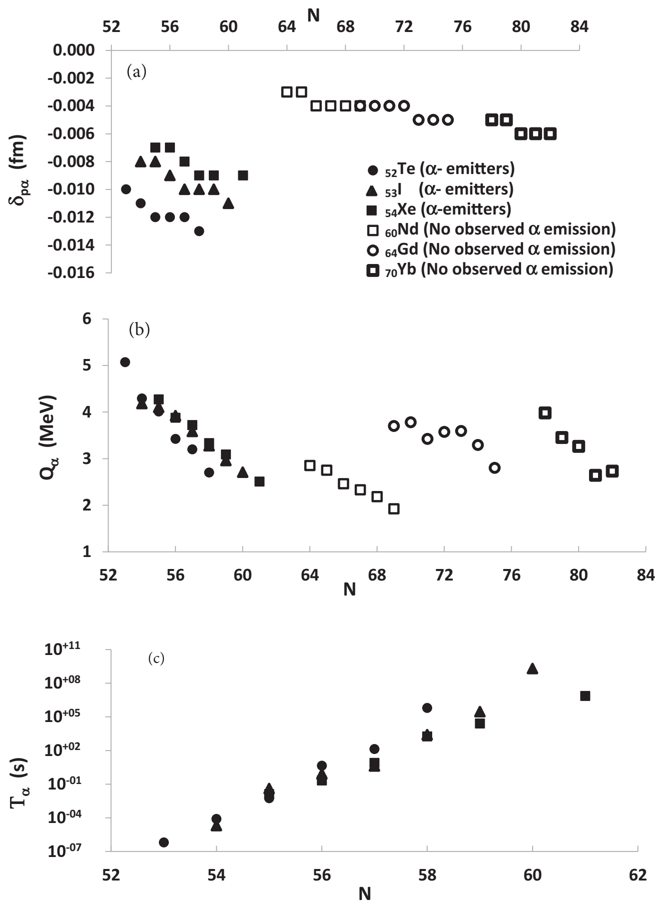

FIG. 1. (a) The difference between the proton skin thickness of the $^{105-110}$Te, $^{107-113}$I, $^{109-113,115}$Xe, $^{124-129}$Nd, $^{133-139}$Gd, and $^{148-152}$Yb isotopes, and in their corresponding daughter (*A*-4, *Z*-2) nuclei, $\delta_{p\alpha} = \Delta_p(A-4, Z-2) - \Delta_p(A,Z)$, as a function of neutron number *N*. (b) The Q_α values (in MeV) [37] for the decays of the isotopes presented in (a). (c) The observed partial half-lives T_α [34] of $^{105-110}$Te, $^{107-113}$I, and $^{109-113,115}$Xe α emitters.

from Δ_n (^{108}Sn) = 0.023 fm to Δ_n (^{115}Sn) = 0.093 fm. The $^{111-119}$Te isotopes presently show no α radioactivity, although they have $Q_\alpha > 0$.

The $^{107-113}$I ($^{109-113,115}$Xe) α-emitters have proton skin thicknesses $\Delta_p = 0.079 - 0.007$ fm ($\Delta_p = 0.082 - 0.011$ fm). The corresponding daughter nuclei exhibit smaller proton skin thicknesses. As seen in Fig. 1(a), the reduction in the proton skin thicknesses due to the α emission increases with *N* (with decreasing Δ_p). For $N = 52 - 58$, the neutron sub-shell $g_{7/2}$ is occupied in the spherical nucleus. This subshell is favored over the subshell with smaller orbital angular momentum in forming the α particle [38,39]. However, the corresponding Q_α values decrease with increasing *N* [Fig. 1(b)] and the observed half-lives progressively increase [Fig. 1(c)]. Whereas the proton skin increases with *Z* of isotones, the reduction of the proton skin due to α emissions decreases [Fig. 1(a)], but remains larger ($\delta_{p\alpha} = -0.013 - -0.007$ fm) than that for nuclei in which the α decay were not observed. In Fig. 1 we present the results for Nd, Gd, and Yb which have proton skins and similar Q_α values but have no observed α decays. The reductions of proton skins in these nuclei are relatively small with respect to those for the Te, I, and Xe isotopes mentioned. The ^{114}Xe ($\Delta_p = 0.022$ fm, $Q_\alpha = 2.719$ MeV) isotope is expected to have an α-decay mode producing ^{110}Te ($\Delta_p = 0.013$ fm) daughter nucleus, but with relatively long partial half-life ($T_\alpha^{\mathrm{cal.}} = 1.916$ years). The total half-life time of ^{114}Xe is 10 s, due to the fast β^+-decay mode. The isotopes $^{114-120,137}$I and $^{116-121,138}$Xe, which have positive Q_α values but do not exhibit α decay, possess neutron skins of calculated thicknesses up to $\Delta_n = 0.205$ fm. The daughter nuclei $^{110-116,133}$Sb and $^{112-117,134}$Te have relatively thick neutron skins. So, the α decay is suppressed with respect to other decay modes.

Just beyond ^{112}Cs and ^{114}Ba, the α emitters are not observed [34]. They appear again starting from ^{144}Nd ($T_\alpha = 2.29 \times 10^{15}$ years). The shortest half-life within this region is for ^{148}Gd ($T_\alpha = 70.9$ years). The α emitters of short half-lives appear starting from ^{149}Tb ($T_\alpha = 4.118$ h). The differences $\delta_{n\alpha}(A,Z) = \Delta_n(A-4, Z-2) - \Delta_n(A,Z)$ between the neutron skin thicknesses of $^{130-139,\,143-149}$Nd ($Q_\alpha > 0$) and $^{135-143,145-152}$Sm ($Q_\alpha > 0$) nuclei and their daughter nuclei in supposed α-decays are presented in Fig. 2(a). The corresponding Q_α values [37] are displayed in Fig. 2(b). Among the known neodymium $^{124-161}$Nd isotopes, only in ^{144}Nd the α decay could be observed. Both ^{144}Nd and its

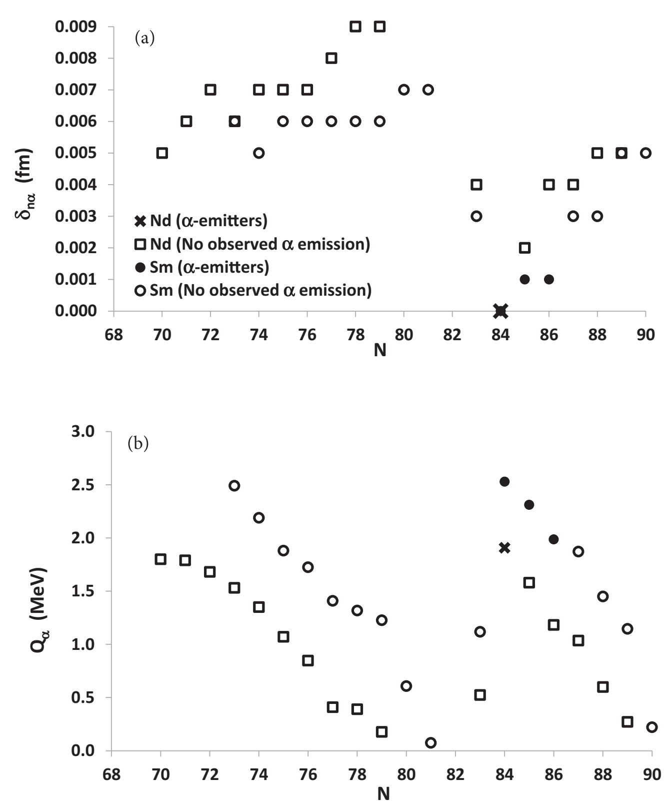

FIG. 2. (a) The difference $\delta_{n\alpha}(A,Z) = \Delta_n(A-4, Z-2) - \Delta_n(A,Z)$ between the neutron skin thickness in the $^{130-139,\,143-149}$Nd ($Q_\alpha > 0$) and $^{135-143,145-152}$Sm ($Q_\alpha > 0$) isotopes and in their possible daughter (*A*-4, *Z*-2) nuclei, as a function of neutron number *N*. (b) The Q_α values [37] for the decays of the isotopes displayed in (a).

daughter ^{140}Ce ($N = 82$) have neutron skin $\Delta_n = 0.115$ fm ($\delta_{n\alpha} = 0$). The $^{124-129}$Nd isotopes have proton skins of $\Delta_p = 0.060 - 0.010$ fm. The decrease $\delta_{p\alpha}$ of the proton skin thickness for their corresponding (A-4, Z-2) nuclei, $^{120-125}$Ce, lies between -0.003 and -0.004 fm [Fig. 1(a)]. The $^{130-139,\ 143,145-149}$Nd ($Q_\alpha > 0$) isotopes have neutron skins with thickness of 0.000–0.165 fm. The corresponding (A-4, Z-2) nuclei show larger neutron skins, $\delta_{n\alpha} > 0$. As shown in Fig. 2, the values of $\delta_{n\alpha}$ for these nuclei lie between 0.002 and 0.009 fm. The $^{135-143,145-152}$Sm isotopes with $Q_\alpha > 0$ have neutron skins 0.003–0.150 fm. Figure 2 shows that larger Q_α and minimal $\delta_{n\alpha}$ are linked together. For $^{146-148}$Sm ($T_\alpha > 6.8$ My), the minimal value of $\delta_{n\alpha} = 0.000 - 0.001$ fm (Fig. 2) correlates with the possibility for observing α decays of these isotopes. The ^{135,136}Sm ($\delta_{n\alpha} \geqslant 0.005$, $T_{\beta^+} \leqslant 47$ s) isotopes have Q_α values comparable to that of $^{146-148}$Sm, but their observed half-lives against β^+ decay are short.

Figure 3(a) shows the neutron skin difference $\delta_{n\alpha}$ versus the corresponding neutron number for the $^{140-155}$Gd isotopes. The heavier isotopes of Gd possess negative Q_α values. In five gadolinium isotopes, $^{148-152}$Gd, α emission has been observed. As seen in Fig. 3(a), the α decay of these parent nuclei leads to a slight increase of the neutron skins in the daughter nuclei $^{144-148}$Sm, $\delta_{n\alpha} = 0.000 - 0.003$ fm. The increase in the neutron skins of the (A-4, Z-2) nuclei corresponding to the other $^{140-147,\ 153-155}$Gd isotopes exhibits larger values of $\delta_{n\alpha}$. The Q_α values, the estimated α-preformation probabilities, and the calculated partial half-lives for the $^{140-155}$Gd isotopes are presented in Figs. 3(b)–3(d), respectively. The experimental partial half-lives [34] for the $^{148-152}$Gd α emitters are also displayed in Fig. 3(d). The preformation probability S_α in Fig. 3(c) is estimated with the empirical expression given in Ref. [40], which accounts for the shell [20] and pairing [23] effects as well as for the difference of the spin-parity assignments of the involved nuclei [24]. The estimated T_α deviates from the experimental data within a factor of 2. If the neutron skins are not taken into account, by considering the same rms radii for both the neutron and proton density distributions, the calculated T_α increases by about one order of magnitude.

Although the nuclei ^{140,141,142}Gd have Q_α close to those for $^{148-152}$Gd in which the α decays were observed and smaller neutron number N, the values of $\delta_{n\alpha}$ for them are relatively large and α decays are strongly hindered. The calculated T_α for ^{140,141,142}Gd, Fig. 3(d), are much larger than their observed half-lives against β^+ decay, $T_{\beta^+} = 14 - 70$ s [34]. Larger Q_α and minimal $\delta_{n\alpha}$ correlate with minimal T_α for the isotopic chain in Fig. 3, indicating the isotopes in which α decays can be easier detect. Comparing the results in Figs. 3(d) and 3(a), we see that the observed T_α are almost proportional to the change $\delta_{n\alpha}$ of the neutron skin thickness. The variation of the displayed half-lives with N is very similar to that of $\delta_{n\alpha}$. The α decay of ^{148}Gd ($N = 84$) to ^{144}Sm ($N = 82$) with $\delta_{n\alpha} = 0$ yields the shortest half-life of Gd isotopes. So, there is a clear tendency of the observed α decays to keep the neutron skin almost unchanged.

The neutron skin difference $\delta_{n\alpha}$ versus N is displayed in Fig. 4 for the $^{147-166}$Ho and $^{153-177}$Yb [Fig. 4(a)], $^{186-224}$Po [Fig. 4(b)], and $^{212-241}$Pa and $^{241-260}$Fm [Fig. 4(c)] isotopes, with $Q_\alpha > 0$. As seen, the α decays of $^{151-154}$Ho and $^{153-158}$Yb result in a slightly larger neutron skin of the daughter nuclei, $\delta_{n\alpha} = 0.000 - 0.004$ fm. Larger changes of the neutron skins, up to $\delta_{n\alpha} = 0.012$ fm, are obtained for $^{147-150,155-166}$Ho and $^{159-177}$Yb, in which the α emission is much less probable. The main conclusion arising from the results presented in Fig. 4(a) is that the α decays are preferably accompanied with relative small increase of the neutron skins in daughter nuclei.

All the known isotopes $^{186-227}$Po, $^{212-241}$Pa, and $^{241-260}$Fm are neutron skinned. As shown in Figs. 4(b) and 4(c), the daughter nuclei after the α decays of $^{186-218}$Po, $^{212-231}$Pa, and $^{241-257}$Fm show $\delta_{n\alpha} = 0.003 - 0.010$ fm. The (A-4, Z-2) nuclei corresponding to other $^{119-224}$Po ($Q_\alpha > 0$), $^{232-241}$Pa, and $^{258-260}$Fm isotopes exhibit larger increases of their neutron skin thicknesses, up to $\delta_{n\alpha} = 0.014$ fm. In these nuclei, the α

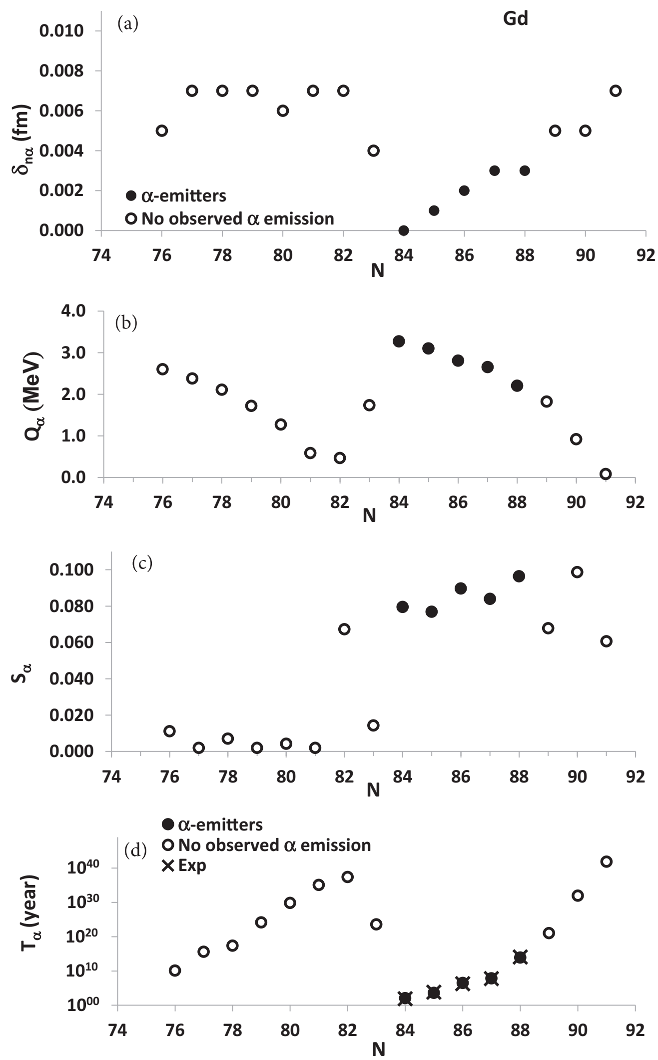

FIG. 3. (a) The same as Fig. 2, but for the $^{140-155}$Gd isotopes. (b) The Q_α values [37]. (c) The estimated α-preformation probability (based on Eq. (10) in Ref. [40]). (d) The calculated partial half-lives, T_α, for $^{140-155}$Gd. The observed partial half-lives T_α [34] for $^{148-152}$Gd are indicated in (d) by crosses.

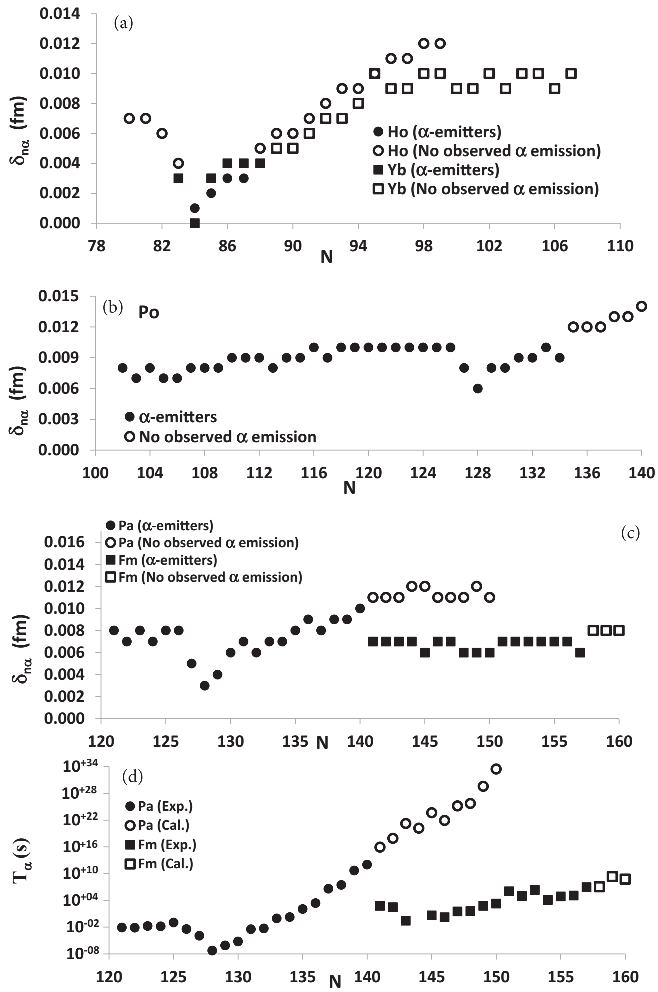

FIG. 4. The same as Fig. 2, but for (a) $^{147-166}$Ho and $^{153-177}$Yb, (b) $^{186-224}$Po, and (c) $^{212-241}$Pa and $^{241-260}$Fm isotopes. (d) The observed partial half-lives T_α [34] of $^{212-231}$Pa and $^{241-257}$Fm α-emitters, and the calculated T_α for the $^{232-241}$Pa and $^{258-260}$Fm nuclei, which have no α emission observed.

emission is relatively hindered. Upon the analysis of the results presented in Figs. 2, 3, and 4, we conclude that the α emission process favors to produce a daughter nucleus exhibiting smallest possible change in its neutron skin thicknesses. The increase of the neutron skin after the α decay would indicate more unstable daughter nucleus. So, this α decay seems to be hindered because the nuclear decay preferably leads to more stable nucleus.

Figure 4(d) displays the experimental partial half-lives of the Pa and Fm α emitters presented in Fig. 4(c), and the calculated partial half-lives of their isotopes having no α-decays observed. The measured half-lives of the $^{212-231}$Pa range from 53 ns to 3.3 $\times$ 10^4 years, while those of $^{241-257}$Fm range from 0.254 s to 100.5 days. Comparing Figs. 4(d) and 4(c), one can clearly see that the half-lives follow to a good extent the changes of the neutron skin thickness. The α decay of ^{219}Pa ($N = 128$) exhibits the minimum $\delta_{n\alpha}$ and the shortest T_α. The calculated T_α of the $^{232-241}$Pa isotopes [Fig. 4(d)] are extremely larger than their observed total half-lives, which lie between $T_{1/2} = 2.27$ min and 1.32 days. Almost constant change of the neutron skin thickness in the α decays of $^{241-257}$Fm is reflected in the narrow range of the half-lives observed. The calculated T_α of $^{258-260}$Fm isotopes are much larger than their detected total half-lives, $T_{1/2} = 370\,\mu\text{s} - 1.5$ s.

IV. CONCLUSIONS

We found that the decays of the proton-skinned α emitters preferably proceed to yield significant decrease in the proton skins of their daughter nuclei. The reduction in the proton skin thicknesses due to the α emission from parent isotopes increases with N (with decreasing their proton skins). The α decay process exhibits very least increase of neutron skin thickness in the produced daughter nuclei, with respect to that of the parent ones. Both the large increase of the neutron skin difference and the slight decrease of the proton skin difference indicate the hindrance of the α decay. This hindrance is reflected in a decrease of both the Q_α value and the α-preformation probability, and very long half-life T_α. For the isotopic chain, the curve pattern of T_α and that of the change of the neutron skin thickness are highly analogous to each other. The values of T_α follow the change of the proton skin thickness. The indicated correlation between T_α and the change of the neutron (proton) skin thickness can be helpful in the study of neutron (proton) skins of radioactive nuclei. It also offers a straightforward method to predict the shorter half-lives against α decays for unknown heaviest nuclei by calculating their proton and neutron densities profiles. Some important estimates of the α-decay characteristics can be obtained without the calculations of interaction potential and preformation factor, but rather calculating only the proton and neutron density profiles if the correlations between them and α decays are established in the isotopic chain. This might trigger further studies of nuclear properties with the self-consistent microscopic methods, which is of great importance for new radioactive beam facilities.

ACKNOWLEDGMENTS

This work was supported by the Academy of Scientific Research and Technology (ASRT, Egypt) and the Joint Institute for Nuclear Research (JINR, Russia).

[1] A. Krasznahorkay *et al.*, Nucl. Phys. A **567**, 521 (1994).
[2] W. M. Seif, Nucl. Phys. A **878**, 14 (2012).
[3] B. A. Brown, Phys. Rev. Lett. **85**, 5296 (2000).
[4] X. Roca-Maza, M. Centelles, X. Viñas, and M. Warda, Phys. Rev. Lett. **106**, 252501 (2011).
[5] C. J. Horowitz and J. Piekarewicz, Phys. Rev. Lett. **86**, 5647 (2001).

[6] J. Piekarewicz, B. K. Agrawal, G. Colò, W. Nazarewicz, N. Paar, P.-G. Reinhard, X. Roca-Maza, and D. Vretenar, Phys. Rev. C **85**, 041302(R) (2012).
[7] H. Sagawa, Phys. Rev. C **65**, 064314 (2002).
[8] J. Piekarewicz, Phys. Rev. C **83**, 034319 (2011).
[9] D. Q. Fang, Y. G. Ma, X. Z. Cai, W. D. Tian, and H. W. Wang, Phys. Rev. C **81**, 047603 (2010).
[10] Guillaume Scamps, Denis Lacroix, G. G. Adamian, and N. V. Antonenko, Phys. Rev. C **88**, 064327 (2013).
[11] G. G. Adamian, N. V. Antonenko, L. A. Malov, G. Scamps, and D. Lacroix, Phys. Rev. C **90**, 034322 (2014).
[12] L. Zamick and N. Auerbach, Nucl. Phys. A **658**, 285 (1999).
[13] P.-G. Reinhard, A. S. Umar, P. D. Stevenson, J. Piekarewicz, V. E. Oberacker, and J. A. Maruhn. Phys. Rev. C **93**, 044618 (2016).
[14] G. G. Adamian, N. V. Antonenko, H. Lenske, S. V. Tolokonnikov, and E. E. Saperstein, Phys. Rev. C **94**, 054309 (2016).
[15] W. M. Seif, M. Ismail, A. I. Refaie, and Laila H. Amer, J. Phys. G: Nucl. Part. Phys. **43**, 075101 (2016).
[16] J. P. Maharana, A. Bhagwat, and Y. K. Gambhir, Phys. Rev. C **91**, 047301 (2015).
[17] W. M. Seif, M. Shalaby, and M. F. Alrakshy, Phys. Rev. C **84**, 064608 (2011).
[18] W. M. Seif, Phys. Rev. C **74**, 034302 (2006).
[19] M. Ismail, W. M. Seif, A. Adel, and A. Abdurrahman, Nucl. Phys. A **958**, 202 (2017).
[20] W. M. Seif, J. Phys. G: Nucl. Part. Phys. **40**, 105102 (2013).
[21] S. Peltonen, D. S. Delion, and J. Suhonen, Phys. Rev. C **75**, 054301 (2007).
[22] Yuejiao Ren and Zhongzhou Ren, Phys. Rev. C **85**, 044608 (2012).
[23] W. M. Seif, Phys. Rev. C **91**, 014322 (2015).
[24] W. M. Seif, M. M. Botros, and A. I. Refaie, Phys. Rev. C **92**, 044302 (2015).
[25] Y. Qian, Z. Ren, and D. Ni, Nucl. Phys. A **866**, 1 (2011).
[26] Peter Mohr, Phys. Rev. C **73**, 031301(R) (2006).
[27] M. Ismail, W. M. Seif, and A. Abdurrahman, Phys. Rev. C **94**, 024316 (2016).
[28] Chang Xu, Zhongzhou Ren, and Jian Liu, Phys. Rev. C **90**, 064310 (2014).
[29] Dongdong Ni and Zhongzhou Ren, Phys. Rev. C **92**, 054322 (2015); **93**, 054318 (2016).
[30] Niu Wan, Chang Xu, and Zhong-Zhou Ren, Nucl. Sci. Tech. **28**, 22 (2017).
[31] P.-G. Reinhard, in *Computational Nuclear Physics*, Vol. 1, edited by K. Langanke, J. A. Maruhn, S. E. Koonin (Springer-Verlag, Berlin, 1990), p. 28.
[32] J. W. Negele and D. Vautherin, Phys. Rev. C **5**, 1472 (1972).
[33] E. Chabanat, E. Bonche, E. Haensel, J. Meyer, and R. Schaeffer, Nucl. Phys. A **635**, 231 (1998).
[34] G. Audi, F.G. Kondev, M. Wang, B. Pfeiffer, X. Sun, J. Blachot, and M. MacCormick, Chin. Phys. C **36**, 1157 (2012).
[35] Jagdish K. Tuli, *Nuclear Wallet Cards*, 8th ed. (2011), Brookhaven National Laboratory, P.O. Box 5000, Upton, New York, 11973-5000, U.S.A. http://www.nndc.bnl.gov/wallet/
[36] L. Bonneau, P. Quentin, and K. Sieja, Phys. Rev. C **76**, 014304 (2007).
[37] M. Wang, G. Audi, A. H. Wapstra, F. G. Kondev, M. MacCormick, X. Xu, and B. Pfeiffer, Chin. Phys. C **36**, 1603 (2012).
[38] H. J. Mang, Phys. Rev. **119**, 1069 (1960)
[39] Chong Qi, Rev. Phys. **1**, 77 (2016).
[40] W. M. Seif, M. Ismail, and E. T. Zeini, J. Phys. G: Nucl. Part. Phys. **44**, 055102 (2017).